Color Tuning of Cyclometalated Iridium Complexes through Modification of Phenylpyrazole Derivatives and Ancillary Ligand Based on ab Initio Calculations

Tae-Hyuk Kwon,[†] Hyo Soon Cho,[†] Myoung Ki Kim,[†] Ji-Whan Kim,[‡] Jang-Joo Kim,[‡] Kwan Hee Lee,[§] Su Jin Park,[§] Ik-Soo Shin,[†] Hasuck Kim,[†] Dong Mok Shin,[†] Young Keun Chung,[†] and Jong-In Hong*[,†]

Department of Chemistry, College of Natural Sciences, Seoul National University, Seoul 151-747, Korea, School of Materials Sciences and Engineering, Seoul National University, Seoul 151-744, Korea, and Corporate R&D Center, Samsung SDI, Suwon 449-902, Korea

Received July 27, 2004

Various iridium complexes consisting of phenylpyrazole (*ppz*) ligands and isoquinolinecarboxylic acids (*iq*) as ancillary ligands were designed by energy band-gap calculations via ab initio calculations and synthesized to give rise to various emission wavelengths as expected. Fine color tuning was achieved through varying the position of the methyl substituent on the phenylpyrazole moiety with HOMO electron densities. Additional color tuning was made possible by altering the LUMO through the use of different ancillary ligands such as 1-isoquinolinecarboxylic acid (1*iq*) and 3-isoquinolinecarboxylic acid (3*iq*).

Introduction

During the past decade, organic light-emitting diodes (OLEDs) were extensively studied for application as next generation flat-panel displays because of their high luminescence, low drive voltage, fast response, and abundant range of colors. Since the strong spin−orbit coupling of heavy metal ions allows for efficient intersystem crossing (ISC) between singlet and triplet excited states, high quantum efficiency can result. Therefore, research on cyclometalated iridium or other heavy metal complexes as dopants for highly efficient OLEDs has received a great deal of attention recently.[1,2,5] In fact, it turns out that cyclometalated iridium complexes are very efficient emissive dopants compared to those used in conventional fluorescent OLEDs.[1,2] However, emission color tuning in phosphorescent OLEDs is still needed to improve color purity and to produce various colors.

To achieve a full-color display, color tuning via fluorescence has been studied for many years.[3] Anzenbacher and other workers reported on a new class of electroluminescent compounds based on AlQ_3 with substituents in which the electronic nature of the substituents affects the emission color of the resulting Al(III) complexes.[3e−i] Kim and co-workers showed that

* To whom correspondence should be addressed. E-mail: jihong@plaza.snu.ac.kr.

[†] Department of Chemistry, Seoul National University.

[‡] School of Materials Sciences and Engineering, Seoul National University.

[§] Samsung SDI.

(1) (a) Baldo, M. A.; O'Brien, D. F.; You, Y.; Shoustikov, A.; Sibly, S.; Thompson, M. E.; Forrest, S. R. *Nature* **1998**, *395*, 151. (b) O'Brien, D. F.; Baldo, M. A.; You, Y.; Shoustikov, A.; Sibly, S.; Thompson, M. E.; Forrest, S. R. *Appl. Phys. Lett.* **1999**, *74*, 442. (c) Baldo, M. A.; Lammansky, S.; Burrows, P. E.; Thompson, M. E.; Forrest, S. R. *Appl. Phys. Lett*. **1999**, *75*, 4. (d) Adachi, C.; Baldo, M. A.; Forrest, S. R.; Thompson, M. E. *Appl. Phys. Lett*. **2000**, *77*, 904. (e) Baldo, M. A.; Adachi, C.; Forrest, S. R. *Phys. Rev. B* **2000**, *62*, 10967. (f) Adachi, C.; Baldo, M. A.; Forrest, S. R.; Lamansky, S.; Thompson, M. E. *Appl. Phys. Lett*. **2001**, *78*, 1622. (g) Lammansky, S.; Diurovich, P.; Murphy, D.; Adbel-Razzaq, F.; Lee, H.-E.; Adachi, C.; Burrows, P. E.; Forrest, S. R.; Thompson, M. E. *J. Am. Chem. Soc*. **2001**, *123*, 4304. (h) Lammansky, S.; Diurovich, P.; Murphy, D.; Adbel-Razzaq, F.; Kwang, R.; Tsyba, I. Bortz, M., Mui, B., Bau, R.; Thompson, M. E. *Inorg. Chem*. **2001**, *40*, 1704.

(2) (a) Adachi, C.; Baldo, M. A.; Thompson, M. E.; Forrest, S. R. *J. Appl. Phys.* **2001**, *90*, 5048. (b) Ikai, M.; Tokito, S.; Sakamoto, Y.; Suzuki, T.; Taga, Y. *Appl. Phys. Lett.* **2001**, *79*, 156. (c) Wang, Y.; Herron, N.; Gruchin, V. V.; Lecoluox, D. D.; Petrov, V. A. *Appl. Phys. Lett*. **2001**, *79*, 449. (d) Adachi, C.; Kwong, C.; Diurovich, P.; Adamovich, V.; Baldo, M. A.; Thompson, M. E.; Forrest, S. R. *Appl. Phys. Lett.* **2001**, *79*, 2082. (e) Grushin, V. V.; Herron, N.; Lecoluox, D. D.; Marshall, W. J.; Petrov, V. A.; Wang, Y. *Chem. Commun.* **2001**, 1494. (f) Books, J.; Babayan, Y.; Lamansky, S.; Djurovich, P. I.; Tsyba, I.; Bau, R.; Thompson, M. E. *Inorg. Chem*. **2002**, *41*, 3055. (g) Tsuzuki, T.; Shirasawa, N.; Suzuki, T.; Tokito, S. *Adv. Mater.* **2003**, *15*, 1455. (h) Tamayo, A. B.; Alleyne, B. D.; Djurovich, P. I.; Lamansky, S.; Tsyba, I.; Ho, N. N.; Thompson, M. E. *J. Am. Chem. Soc.* **2003**, *125*, 7377. (i) Tsuboyama, A.; Iwawaki, H.; Furogori, M.; Mukaide, T.; Kamatani, J.; Igawa, S.; Moriyama, T.; Mura, S.; Takiguchi, T.; Okada, S.; Hoshino, M.; Ueno, K. *J. Am. Chem. Soc.* **2003**, *125*, 12971. (j) Li, J.; Djurovich, P. I.; Alleyne, B. D.; Tsyba, I.; Ho, N. N.; Bau, R.; Thompson, M. E. *Polyhedron* **2004**, *23*, 419.

(3) (a) Joshi, H. S.; Jamshidi, R.; Tor, Y. *Angew. Chem., Int. Ed.* **1999**, *38*, 2772. (b) Meng, H.; Huang, W. *J. Org. Chem.* **2000**, *65*, 3894. (c) Mori, A.; Sekiguchi, A.; Masui, K.; Shimada, T.; Horie, M.; Oskada, K.; Kawamoto, M.; Ikeda, T. *J. Am. Chem. Soc.* **2003**, *125*, 1700. (d) Hwang, G. T.; Son, H. S.; Ku, J. K.; Kim, B. H. *J. Am. Chem. Soc*. **2003**, *125*, 11241. (e) Pohl, R.; Anzenbacher, P., Jr. *Org. Lett.* **2003**, *5*, 2769. (f) Pohl, R.; Montes, V. A., Shinar, J., Anzenbacher, P., Jr. *Org. Lett.* **2004**, *6*, 1723. (g) Chen, T.-M., Laskar, I. R. *Chem. Mater.* **2004**, *16*, 111. (h) Meyers, M.; Weck, M. *Chem. Mater.* **2004**, *16*, 1183. (i) Pohl, R.; Montes, V. A.; Shinar, J.; Anzenbacher, P., Jr. *J. Org. Chem.* **2004**, *69*, 1723.

(4) (a) Steel, P. J.; Lahouses, F.; Lerner, D.; Marzin, C. *Inorg. Chem*. **1983**, 22, 1488 (b) Steel, P. J.; Constable, E. C. *J. Chem. Soc., Dalton Trans*. **1990**, 1389. (c) Adamovich, V. I.; Cordero, S. R.; Djurovich, P. I.; Tamayo, A.; Thompson, M. E.; D'Andrade, B. W.; Forrest, S. R. *Org. Electron*. **2003**, *4*, 77.

(5) (a) Nazeeruddin, M. K.; H−Baker, R.; Berner, D.; Rivier, S.; Zuppiroli, L.; Graetzel, M.*J. Am. Chem. Soc.* **2003**, *125*, 8790. (b) Lu, Wei.; Mi, B.-X.; Chan, M. C. W.; Hui, Z.; Che, C.-M.; Zhu, N.; Lee, S.-T. *J. Am. Chem. Soc.* **2004**, *126*, 4958.

10.1021/om049419e CCC: $30.25
Publication on Web 02/25/2005

the fluorescence of bis-enediynes can be tuned through the modification of their core and peripheral units.[3d] However, color tuning via phosphorescence has only recently been studied and there are few existing reports in the literature.[1h,2d,h,i,3d,5] For example, Thompson's group investigated ligand tuning of phosphorescence based on iridium complexes with benzothiazole and benzoxazole through the differences in the polarizabilty and the basicity of sulfur relative to oxygen.[1g] They have achieved color tuning through the substitution of various electron-withdrawing groups at the phenylpyridine ligand of iridium complexes[2d] and also developed an ancillary ligand that can lead to blue-shifted emissions.[2j] Many cyclometalated homoleptic iridium complexes and heteroleptic iridium complexes with phenylpyridine ligands have been reported in the literature.[1,2,5,6] However, only few heteroleptic iridium complexes with *ppz* ligands have been studied,[4c] although pyridyl and pyrazole groups have similar electronic and coordinating characteristics.[4a,b] There are few reports for color tuning via ancillary ligand change.[1g,2j,5b]

In this study, we have designed heteroleptic iridium complexes with *ppz* ligands and *iq* ancillary ligands as tunable phosphors, where their emission wavelengths are easily controlled through modification of their HOMO and LUMO electron densities. In other words, fine color tuning has been achieved through subtle changes in the structure of phenylpyrazole and ancillary ligands.

We obtained the HOMO−LUMO energy orbitals of compounds $(ppz)_2$Ir3*iq* and $(ppz)_2$Ir1*iq* using an ab initio calculation (DFT/B3LYP), which would provide a method to achieve color tuning via structural modification on the ligand (Figure 1).[11] The advantage of this system is the relative ease with which the emission wavelength can be controlled by changing HOMO−LUMO electron densities. This is because the HOMO electron densities are located on the *ppz* ligand and iridium, while the LUMO electron densities are located on the *iq* ligand, which acts as an emitting mode (Figure 1). If the electron densities of HOMO and LUMO exist in the same position, it is difficult to predict and control the emission energy because of the simultaneous energy change of both HOMO and LUMO upon the structural modification.[2f,h,6] Therefore, the emission wavelengths of $(ppz)_2$Ir*iq* complexes are easily controlled.

First, we wanted to control the phosphorescent emission wavelength of iridium complexes by varying both the position and the number of methyl substituents on the *ppz* ligand, which would affect the HOMO energy. According to a DFT calculation, 1*iq* has more stable LUMO energy than 3*iq* (Table 2).[11] Therefore, we expected that the color could also be tuned by employing different ancillary ligands such as 3*iq* and 1*iq*. In this manner, we were able to control the LUMO energy.

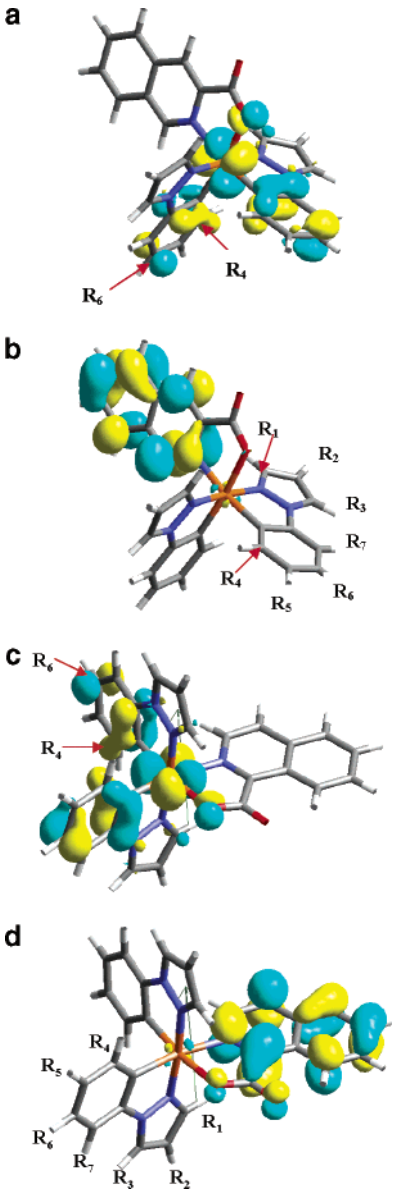

Figure 1. HOMO−LUMO energy orbitals of both $(ppz)_2$-Ir3*iq* and $(ppz)_2$Ir1*iq* through ab initio calculation (DFT/B3LYP). (a) $(ppz)_2$Ir3*iq* HOMO energy orbitals, (b) $(ppz)_2$Ir3*iq* LUMO energy orbitals, (c) $(ppz)_2$Ir1*iq* HOMO energy orbitals, (d) $(ppz)_2$Ir1*iq* LUMO energy orbitals

Results and Discussion

Synthesis of Ligands and Ir Complexes The *ppz* derivatives were easily synthesized via the Buchwald method as shown in Scheme 1.[7]

To a mixture of CuI, pyrazole derivatives, and K_3PO_4 in dioxane (or toluene) were successively added aryl halide and (±)-*trans*-1,2-diaminocyclohexane under nitrogen. The reaction tube was quickly sealed, and the contents were stirred while being heated in an oil bath at 110 °C for 24 h. The crude product was extracted with ethyl acetate and purified by column chromatography.

(6) (a) Hay, P. J. *J. Phys. Chem. A* **2002**, *106*, 1634. (b) Jung, S. O.; Kang, Y.; Kim, H.-S.; Kim, Y.-H.; Yang, K.; Kwon, S.-K. *Bull. Kor. Chem. Soc.* **2003**, *24*, 1521.

(7) (a) Klapars, A.; Antillar, J. C.; Huang, X.; Buchwald, S. L. *J. Am. Chem. Soc.* **2001**, *123*, 7727. (b) Antillar, J. C.; Huang, X.; Klapars, A.; Buchwald, S. L. *J. Am. Chem. Soc.* **2002**, *124*, 11684.

(8) (a) Nonoyama, M. *Bull. Chem. Soc. Jpn.* **1974**, *47*, 767. (b) Lamansky, S.; Djurovich, P.; Murphy, D.; Abdel-Razaq, F.; Kwong, I.; Tsyba, R.; Bortz, M.; Mui, B.; Bau, R.; Thompson, M. E. *Inorg. Chem.* **2001**, *40*, 1704.

(9) Vincente, J.; Arcas, A.; Bautista, D.; Arellano, M. C. R. de. *J. Organomet. Chem.* **2002**, *663*, 164.

(10) Whitaker, J. *Electronic Displays: Technology, Design, and Application*; McGraw-Hill: New York, 1994; p 92.

(11) DFT calculations were performed at the B3LYP level. Basis set: Ir (Stuttgart ECP) and CHON (6-31G). The HOMO and LUMO energies were determined after geometry optimization via the DFT method. The meridional-like structures were modeled based on the X-ray crystal structures. See the Supporting Information for detailed calculations.

Table 1. Selected Bond Distances and Bond Angles for (*ppz*)$_2$Ir3*iq* (1) and (4*mppz*)$_2$Ir1*iq* (11)

bond type	(*ppz*)$_2$Ir3*iq* (**1**)	(4*mppz*)$_2$Ir1*iq* (**11**)
	Bond Distances (Å)	
Ir−N1	2.147(3)	2.134(4)
Ir−N2	2.027(4)	2.034(4)
Ir−N4	2.008(3)	2.015(5)
Ir−O1	2.153(3)	2.157(3)
Ir−C15	2.017(4)	2.019(5)
Ir−C24	2.003(4)	2.009(5)
	Bond Angles (deg)	
C(24)−Ir(1)−C(15)	89.91(16)	87.0(2)
C(24)−Ir(1)−N(2)	93.75(15)	96.8(2)
C(15)−Ir(1)−N(1)	170.22(14)	174.16(18)
C(24)−Ir(1)−O(1)	174.62(15)	172.76(17)
C(15)−Ir(1)−O(1)	93.07(14)	98.62(16)
N(2)−Ir(1)−O(1)	91.18(12)	88.66(15)
N(1)−Ir(1)−O(1)	77.51(11)	75.91(15)

Table 2. Comparison of Experimental vs Calculated (DFT) Emission Wavelengths (λ_{em}) and Electrochemical Data for Iridium Complexes 1−16

compd	λ_{em}/nm (calc)[a]	E_g/eV[b]	compd	λ_{em}/nm (calc)	E_g/eV[b]
1	532 (532)	2.87	**9**	574	
2	544 (550)		**10**	587 (592)	
3	537 (537)	2.84	**11**	575	2.68
4	555	2.80	**12**	599	2.53
5	542 (540)		**13**	582	
6	553 (543)		**14**	594	
7	540 (541)		**15**	577	
8	558	2.75	**16**	603 (597)	2.49

[a] 30 nm was added to the calculated DFT values for trend comparison purposes with the experimental data. See the Supporting Information. [b] All potentials were determined at room temperature in acetonitrile solutions (0.1 M n-Bu_4PF_6) vs AgQRE. Electrochemical data of compounds **8** and **12** were obtained at a scan rate of 1 V/s and those of the others at 0.2 V/s. $E_{HOMO} = E^{1/2}_{ox} + 4.49$ eV and $E_{LUMO} = E^{1/2}_{red} + 4.49$ eV. Electrochemical band gaps were determined using $E_g = E_{HOMO} - E_{LUMO}$. More detailed data can be found in the Supporting Information.

Scheme 1. Synthesis of Phenylpyrazole (*ppz*) Derivatives

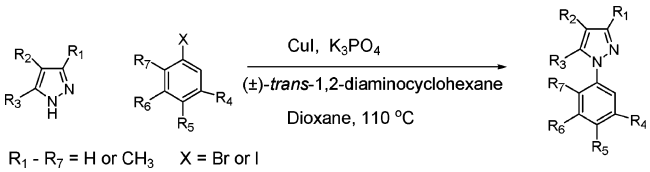

The cyclometalated iridium complexes were synthesized according to the general procedure as reported in the literature (Scheme 2).[1g,8] Cyclometalated Ir(III) μ-chloro-bridged dimers of general formula C$\wedge N_2$Ir(μ-Cl)$_2$IrC$\wedge N_2$ were synthesized according to a modified version of the Nonoyama procedure,[8a] by refluxing $IrCl_3 \cdot nH_2O$ with 2−2.5 equiv of cyclometalating ligand in a 3:1 mixture of 2-methoxyethanol and water for 6−7 h.

The reaction mixture was cooled to room temperature, and more water was added to precipitate the product. The resulting mixture was subsequently filtered through a Büchner funnel and then washed with hexane and ethyl ether several times to provide the crude product. A mixture of the chloro-bridged dimer crude product, 3 equiv of isoquinolinecarboxylic acid, and 10−15 equiv of sodium carbonate was refluxed in an inert atmosphere in 2-ethoxyethanol for 4−5 h. After cooling to room temperature, the solvent was evaporated in high vacuum and dissolved in methylene chloride. The organic phase was washed with water and dried over

Scheme 2. Synthesis of (*ppz*)$_2$Ir3*iq* (1) and (*ppz*)$_2$Ir1*iq* (9)

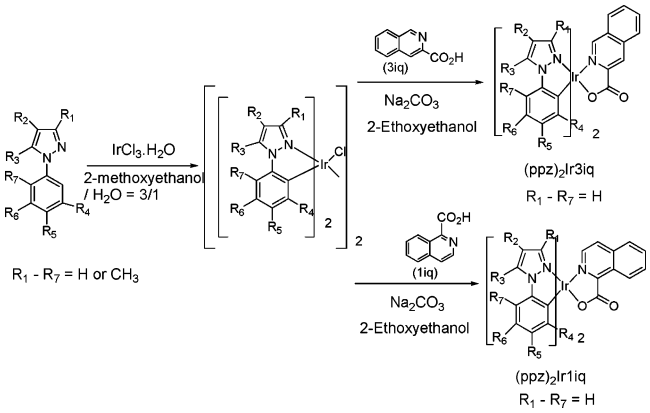

Na_2SO_4. The solvent was evaporated to give the crude product, which was applied to column chromatography on silica gel, followed by eluting with methylene chloride, ethyl acetate, and methyl alcohol to provide the desired product. Figure 2 shows the various iridium complexes prepared according to Scheme 1 and Scheme 2. The structure of these compounds with ancillary ligands is different from the iridium tris-chelate compound.[2h]

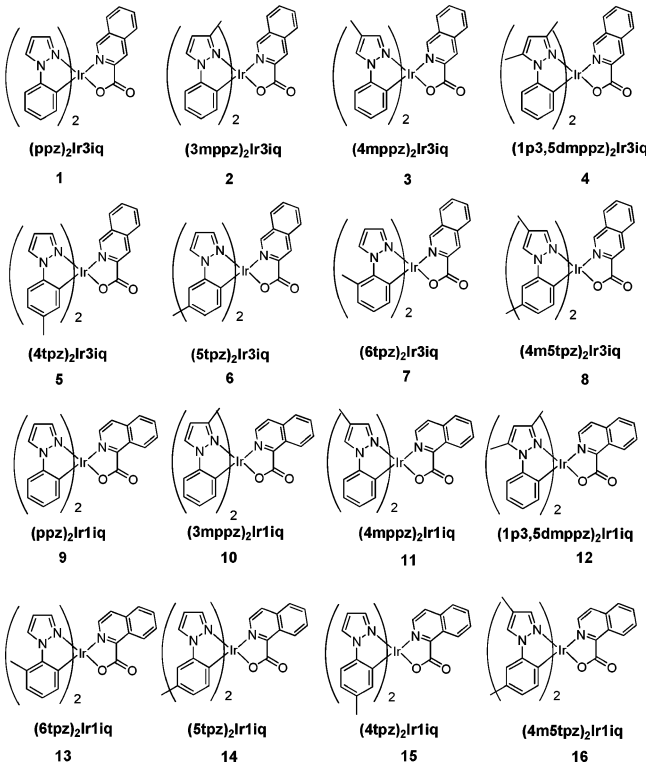

Figure 2. Various iridium complexes.

X-ray Crystallography These heteroleptic compounds exist only in a meridional-like structure—the nitrogen part of one *ppz* ligand *trans* to a π-acceptor N atom in the adjacent *ppz* ligand and the nitrogen part of the *iq* ligand *trans* to the σ-donor C atom in the adjacent *ppz* ligand—as shown in Figure 3,[1i,2j] whereas iridium tris-chelate compounds can have both facial and meridional structures.[2h] That is, the complex exhibits an octahedral coordination geometry around Ir and

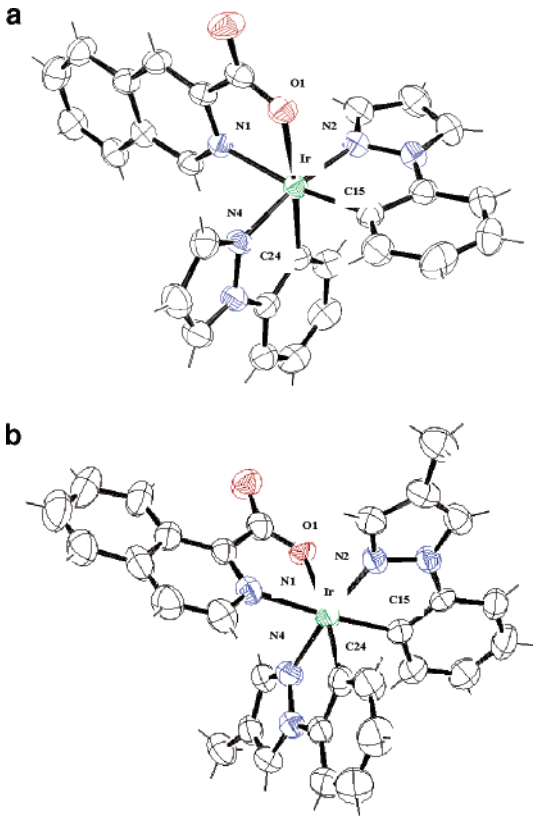

Figure 3. ORTEP drawing of $(ppz)_2$Ir3*iq* (**1**) and $(4mppz)_2$Ir1*iq* (**11**). The thermal ellipsoids for the image represent the 30% probability limit. (a) $(ppz)_2$Ir3*iq* (**1**), (b) $(4mppz)_2$Ir1*iq* (**11**).

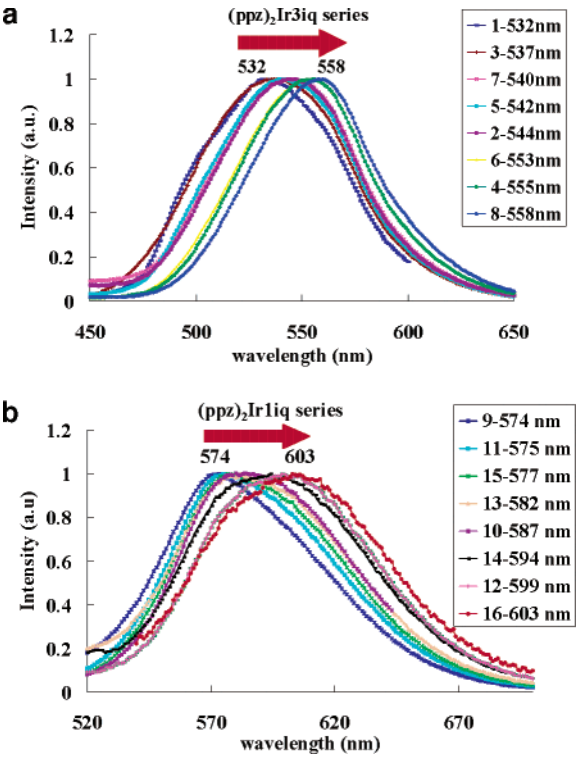

Figure 4. Fine color tuning through the substitution on the phenylpyrazole: (a) emission wavelength (λ_{em}/nm) of $(ppz)_2$Ir3*iq* series, (b) emission wavelength (λ_{em}/nm) of $(ppz)_2$Ir1*iq* series. Numbers (in nm) after the compound numbering in insets are wavelengths of the maximum emission intensity.

prefers a *cis*-C,C *trans*-N,N chelate arrangement to *trans*-C,C *trans*-N,N chelate. Electron-rich σ-phenyl ligands usually display a very strong *trans* effect. Therefore, the *trans* C−C arrangement is expected to be thermodynamically higher in energy and thus kinetically more labile.[3d] This well-known phenomenon has been recently referred to as "transphobia".[3d,9] The Ir−O bond length (2.153 and 2.157 Å) is longer than the mean Ir−O bond length (2.088 Å) reported, and this observation reflects large *trans* influence of the phenyl group.[1i,3d,6] The Ir−N1 bond length (2.134 Å) observed in $(4mppz)_2$Ir1*iq* is slightly shorter than Ir−Nl bond length of $(ppz)_2$Ir3*iq* (2.147 Å). This would imply *trans* influence of the phenyl group on the 4*mppz* ligand. Presumably, this *trans* effect stabilizes the LUMO energy of $(4mppz)_2$Ir1*iq* more than that of $(ppz)_2$Ir3*iq* because the electron density of the LUMO is concentrated in the *iq* ancillary ligand.

The bond lengths of Ir−N1 (2.134 and 2.147 Å) *trans* to the *ppz* phenyl are similar to those of the Ir−N bonds (2.117−2.135 Å) of the facial isomer of the iridium tris-chelate compound with the *ppz* ligand.[2h] Likewise, the mutually *trans* Ir−N bond lengths (Ir−N2 and Ir−N4 bond lengths range from 2.008 to 2.034 Å) are similar to those of the Ir−N bonds (2.013−2.026 Å) of the meridional isomer of the iridium tris-chelate compound with the *ppz* ligand.[2h] Also the Ir−N1 bond lengths (2.147 and 2.134 Å) are longer than the Ir−N2 (2.027 and 2.034 Å) and the Ir−N4 (2.008 and 2.015 Å) bond lengths due to the *trans* effect. The Ir−C15 bond lengths (2.017 and 2.019 Å) of these complexes are similar to those of the Ir−C bond lengths (2.015−2.027 Å) of the facial iridium tris-chelate compound with the *ppz* ligand.[2h]

Color Tuning Based on DFT Calculation. On the basis of DFT calculations,[11] the HOMO is concentrated at positions R_4 and R_6 of the *ppz* ligand and the iridium moiety (Figure 1). Therefore, if electron-donating groups (EDGs) are attached at these positions, one would expect a dramatic change in energy due to the destabilization of the HOMO. Substituting methyl groups on the remaining positions (R_1−R_3, R_5, and R_7) of the *ppz* ligand would cause a small change in their emission wavelengths. Substitution of more methyl groups on the *ppz* ligand would cause a larger red shift in emission spectra. It turns out that this expectation correlates well with the emission data (Figure 4 and Table 2).

Complex **6** (λ_{max} = 553 nm), which has a methyl substitutent at the R_6 position, shows a dramatic change of emission wavelength (a red shift of 21 nm) compared to the unsubstituted complex **1** (λ_{max} = 532 nm). Two methyl-substituted *ppz* complexes—**4** (λ_{max} = 555 nm) and **8** (λ_{max} = 558 nm)—show a red shift to a wavelength ca. 25 nm larger than that for the unsubstituted *ppz* complex **1** (λ_{max} = 532 nm).

According to DFT calculations (Figure 1 and Table 2), fine color tuning can be achieved through varying the position of substituents on the *ppz*. Iridium complexes with methyl substituents on the positions with no electron density clouds show smaller red shifts—**2** (λ_{max} = 544 nm), **5** (λ_{max} = 542 nm), **7** (λ_{max} = 540 nm), and **3** (λ_{max} = 537 nm)—compared to **6** (λ_{max} = 553 nm), where the electron density is concentrated on the R_6

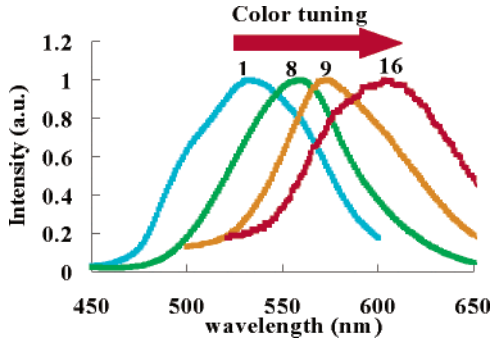

Figure 5. Color tuning through the exchange of the ancillary ligand (0.02 mM solution of CH_2Cl_2).

position. Complex **3** (λ_{max} = 537 nm) places the methyl substituent at the R_2 position on the *ppz* ligand, which is located furthest away from the HOMO. This would constitute a plausible reason for its small red shift. Position R_2 on the *ppz* ligand would be an ideal place to introduce a functionality with other properties such as thermal stability without causing any color change. The (*ppz*)$_2$Ir1*iq* series also show the same trend.

Therefore, we conclude that substitution at the position where the electron densities are concentrated in the HOMO has a pronounced effect on its emission wavelength. The greater the number of substituted methyl groups on the *ppz* ligand, the larger the red shift when compared to the unsubstituted *ppz* complex. Since substitution with an EDG on the position with the HOMO electron density causes a red shift, we expect that substitution with an electron-withdrawing group would possibly cause a blue shift.

Color tuning can also be achieved by using a different ancillary ligand such as two structural isomers—3*iq* and 1*iq* (Figure 5). This is supported by ab initio calculations and electrochemical studies via cyclic voltammety (Table 2). The electrochemical data are in accordance with the electronic spectroscopy results and DFT calculations. For example, through this structural change from 3*iq* to 1*iq*, the energy gap (E_g) between the HOMO and LUMO is reduced when compound **2** (HOMO −5.00, LUMO −1.98, E_g 3.02 eV, triplet state 2.34 eV) is compared with compound **10** (HOMO −5.00, LUMO −2.09, E_g 2.91 eV, triplet state 2.21 eV) through the DFT calculation,[11] and also the energy gap (E_g) via cyclic voltammetry is gradually reduced from compound **1** (2.87 eV) to compound **16** (2.49 eV) (Table 2).

This difference accounts for the fact that complex **1** (λ_{max} = 532 nm) displays a green color (CIE 0.38, 0.57) as opposed to the reddish-yellow color (CIE 0.44, 0.44) of **9** (λ_{max} = 574 nm). Therefore, a red color can be obtained by using the dimethylphenylpyrazole ligand along with a 1*iq* ancillary ligand as shown in **16** (CIE 0.56, 0.43). Figure 6 shows the Commission Internationale de L'Eclairage (CIE) chromaticity coordinate from a 0.02 mM solution of various iridium complexes (**1**, **8**, **9**, and **16**) in CH_2Cl_2.[10]

Quantum Efficiency and Phosphorescence Lifetime. The quantum efficiency measurements were carried out at room temperature in degassed dichloromethane solution (Table 3). A solution of Ir(ppy)$_3$ (Φ_{PL} = 0.40 in 2-methyltetrahydrofuran) was used as reference.[2f,h] All complexes show very weak emission at room temperature (Φ_{PL} < 0.2%), but are intensely

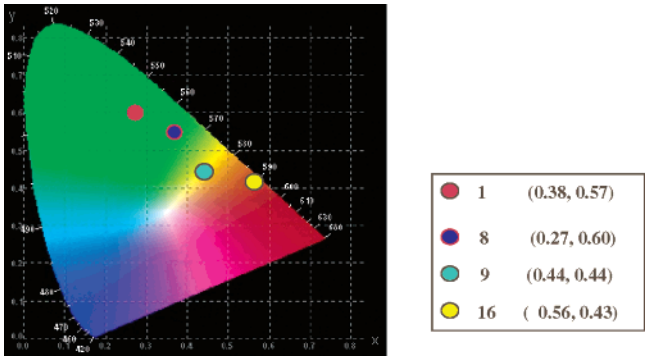

Figure 6. CIE chromaticity coordinate from 0.02 mM solution of various iridium complexes in CH_2Cl_2.

Table 3. Quantum Efficiencies and Phosphorescence Lifetimes

compd	Φ_{PL}[a]	τ (μs)[b]	compd	Φ_{PL}[a]	τ (μs)[b]
1	0.06	8.5	**9**	0.02	0.28
2	0.09	5.0	**10**	0.011	0.27
3	0.07	6.9	**11**	0.018	0.27
4	0.14	4.2	**12**	0.009	0.22
5	0.09	7.1	**13**	0.018	0.24
6	0.11	4.0	**14**	0.009	0.19
7	0.08	6.3	**15**	0.013	0.20
8	0.10	2.7	**16**	0.009	0.16

[a] Quantum efficiency measurements were carried out at room temperature (298 K) in CH_2Cl_2 solution. Solution of Ir(ppy)$_3$ (φ = 0.40 in 2-methyltetrahydrofuran) was used as reference.[2f,h] [b] Phosphorescence lifetime measurements were performed at room temperature in 1% PMMA film.

luminescent at 77 K (see the Supporting Information). Several related *ppz* cyclometated Ir, Pt, and Rh complexes have also been reported to be poorly emissive in solution but highly emissive in glassy matrixes at 77 K.[2h,12] Correlation between quantum effciency and phosphorescence lifetime was reported by the Thompson group.[2h,13] Shorter lifetime and stronger *trans* effect would cause lower quantum efficiency in the isomer complexes. Similar trends are observed in *iq* complexes. The 3*iq* complexes have longer emission decay lifetimes and, concomitantly, much larger luminescence efficiencies than the 1*iq* complexes. The Ir−N1 bond in the 1*iq* complexes is shorter than in the *3iq* complexes because of the *trans* effect of the phenyl group on the 4*mppz* ligand. These results well coincide with the fact that 1*iq* complexes have lower quantum efficiencies than 3*iq* complexes. Assuming that the emitting state of a complex is formed with unit efficiency, one can calculate the radiative (k_r) and nonradiative (k_{nr}) rate constants.[2h] The 3*iq* and 1*iq* complexes have similar radiative constants (k_r), but nonradiative rate constants (k_{nr}) for the 1*iq* complexes are more than an order of magnitude larger than those of the 3*iq* complexes (Table 4), as can be expected from the lower quantum efficiencies of the 1*iq* complexes.

(12) (a) Sandrini, D.; Maestri, M.; Ciano, M.; Balzani, V.; Lueoend, R.; Deuschel-Cornioley, C.; Chassot, L.; Von Zelewsky, A. *Gazz. Chim. Acta* **1988**, *118*, 661. (b) Maeder, U.; Stoeckli-Evans, H.; von Zelewsky, A. *Helv. Chim. Acta* **1992**, *75*, 1320.

(13) For example, the nonradiative rate constant for *mer*-Ir(ppy)$_3$ is more than an order of magnitude larger than that of *fac*-Ir(ppy)$_3$. The mutually *trans* Ir−C bonds in *mer*-Ir(ppy)$_3$ are significantly longer and *trans* Ir−N bonds in *mer*-Ir(ppy)$_3$ are shorter than *fac*-Ir(ppy)$_3$ as a result of the strong *trans* influence of the phenyl groups. Therefore, *fac*-Ir(ppy)$_3$ shows higher quantum efficiency and longer lifetime than *mer*-Ir(ppy)$_3$.

Table 4. Radiative and Nonradiative Decay Rates at Room Temperature

compd	k_r[a]	k_{nr}[b]	compd	k_r[a]	k_{nr}[b]
1	7.1×10^3	1.1×10^5	**9**	7.1×10^4	2.8×10^5
2	1.8×10^4	1.8×10^5	**10**	4.1×10^4	3.7×10^6
3	1.0×10^4	1.3×10^5	**11**	6.7×10^4	3.7×10^6
4	3.3×10^4	2.0×10^5	**12**	4.1×10^4	4.5×10^6
5	1.3×10^4	1.3×10^5	**13**	7.5×10^4	4.1×10^6
6	2.8×10^4	2.3×10^5	**14**	4.7×10^4	5.2×10^6
7	1.3×10^4	1.5×10^5	**15**	6.5×10^4	4.9×10^6
8	3.7×10^4	3.3×10^5	**16**	5.6×10^4	6.2×10^6

[a] $k_r = \Phi_{PL}/\tau$. [b] $\Phi_{PL} = k_r/(k_r + k_{nr})$, $k_{nr} = k_r(1 - \Phi_{PL})/\Phi_{PL}$.

Conclusion

We have designed heteroleptic iridium complexes with phenylpyrazole (*ppz*) and isoquinolinecarboxylic acid (*iq*) as tunable phosphors, where their emission wavelengths are easily controlled through modification of their HOMO and LUMO electron densities. This study shows that the prediction of the HOMO and LUMO energies via ab initio calculation (DFT/B3LYP) is a very important tool for tuning the color, and color fine tuning can be achieved by substituting a methyl group on the *ppz* main ligand and using a different ancillary ligand such as 3-isoquinolinecarboxylic acid (3*iq*) and 1-isoquinolinecarboxylic acid (1*iq*). A DFT calculation correlates well with experimental data. Efforts toward the development of blue color complexes using different substituents are currently underway.

Experimental Section

^{1}H and ^{13}C NMR spectra were recorded using an Advance 300 Bruker spectrometer in chloroform-d_6, CD_3OD, acetone-d_6, or DMSO-d_6. ^{1}H NMR chemical shifts in $CDCl_3$ were referenced to $CHCl_3$ (7.27 ppm), and ^{13}C NMR chemical shifts in $CDCl_3$ were reported relative to $CHCl_3$ (77.23 ppm). UV−visible spectra were recorded on a Beckman DU650 spectrophotometer. Mass spectra were obtained using a QUATTRO LC triple quadrupole tandem mass spectrometer and are reported in units of mass to charge (*m/z*). Phosphorescence lifetime measurements were performed on a Continuum Surelite II-10 and measured by photomultiplier tube through a monochromator by exciting the sample at the third harmonic (355 nm) of a Q-switched Nd:YAG laser with a pulse duration of 7 ns and a repetition rate of 10 Hz at room temperature. Fluorescence spectra were recorded on a Jasco FP-750 spectrophotometer. Analytical thin-layer chromatography was performed using Kieselgel 60F-254 plates from Merck. Column chromatography was carried out on Merck silica gel 60 (70−230 mesh). All solvents and reagents were commercially available and used without further purification unless otherwise noted.

Synthesis of Phenylpyrazole Derivatives (Scheme 1). Phenylpyrazole derivatives were synthesized via the Buchwald method.[7] To a screw-cap test tube were added CuI (5 mol %), pyrazole derivatives (1.2 mmol), K_3PO_4 (2.1 mmol), and toluene (1 mL) followed by nitrogen bubbling for 10−20 min. Bromobenzene derivatives (1.0 mmol) and (±)-*trans*-1,2-diaminocyclohexane (10 mol %) were then successively added under a stream of nitrogen. The reaction tube was quickly sealed, and the contents were stirred while being heated in an oil bath at 110 °C for 24 h. The reaction mixture was cooled to ambient temperature, diluted with ethyl acetate (2−3 mL), and filtered through a plug of silica gel, eluting with additional ethyl acetate (10−20 mL). The filtrate was concentrated, and the resulting residue was purified by column chromatography (methylene chloride) to provide the desired product.

Synthesis of Iridium Complexes (Scheme 2). All synthetic procedures involving Ir(III) species were carried out in an inert gas atmosphere. Cyclometalated Ir(III) μ-chloro-bridged dimers of general formula C∧N_2Ir(μ-Cl)$_2$IrC∧N_2 were synthesized according to a modified version of the Nonoyama procedure, [8] by refluxing $IrCl_3 \cdot nH_2O$ with 2−2.5 equiv of cyclometalating ligand in a 3:1 mixture of 2-methoxyethanol and water for 6−7 h. The reaction mixture was cooled to room temperature, and more water was added to precipitate the product. The resulting mixture was subsequently filtered through a Büchner funnel and then washed with hexane and ethyl ether several times to provide the crude product. The chloro-bridged dimer crude product (0.08 mmol), 0.25 mmol of 3-isoquinolinecarboxylic acid, and 1 mmol of sodium carbonate were refluxed in an inert atmosphere in 2-ethoxyethanol for 4−5 h. After cooling to room temperature, the solvent was evaporated in high vacuum and dissolved in methylene chloride. The organic phase was washed with water and dried over Na_2SO_4. The solvent was evaporated to give the crude product, which was applied to column chromatography on silica gel, eluting with methylene chloride and methyl alcohol to provide the desired product.

(*ppz*)$_2$Ir3*iq* (1). ^{1}H NMR (300 MHz, $CDCl_3$): δ (ppm) 9.41 (s, 1H), 8.69 (s, 1H), 8.15−8.06 (m, 4H), 7.86−7.80 (m, 4H), 7.12 (d, J = 6.0 Hz, 2H), 6.78 (t, J = 7.5 Hz, 2H), 6.66 (t, J = 3.0 Hz, 2H), 6.54 (t, J = 8.9 Hz, 2H), 6.02 (d, J = 6.0 Hz, 2H). ^{13}C NMR (300 MHz, $CDCl_3$): δ (ppm) 174.06, 152.16, 145.34, 143.96, 143.86, 138.37, 137.36, 135.77, 134.61, 134.40, 132.45, 131.19, 130.34, 129.78, 128.88, 128.61, 127.79, 126.55, 126.40, 126.27, 126.02, 126.01, 122.35, 122.02, 111.22, 111.00, 107.58, 107.46. ESI-MS: *m/z* 652.6 [M + H$^+$]. Anal. Calcd for $C_{28}H_{20}IrN_5O_2 \cdot H_2O$: C 50.29; H 3.32; N 10.47. Found: C 50.75; H 3.30; N 10.18.

(3*mppz*)$_2$Ir3*iq* (2). ^{1}H NMR (300 MHz, $CDCl_3$): δ (ppm) 8.81 (s, 1H), 8.46 (s, 1H), 8.07 (d, J = 12 Hz, 1H), 8.03 (d, J = 3.0 Hz, 2H), 7.89−7.80 (m, 2H), 7.73−7.69 (m, 1H), 7.24−7.12 (m, 2H), 7.01 (t, J = 4.5 Hz, 1H), 6.90 (t, J = 4.5 Hz, 1H), 6.88 (t, J = 4.5 Hz, 1H), 6.72 (t, J = 4.5 Hz, 1H), 6.50 (d, J = 6.0 Hz, 1H), 6.31 (d, J = 6.0 Hz, 1H), 6.29−6.21 (m, 2H) 2.49 (s, 3H), 1.58 (s, 3H). ESI-MS: *m/z* 680.5 [M + H$^+$]. Anal. Calcd for $C_{30}H_{24}IrN_5O_2$: C 53.09; H 3.56; N 10.32. Found: C 53.03; H 3.61; N 9.54.

(4*mppz*)$_2$Ir3*iq* (3). ^{1}H NMR (300 MHz, $CDCl_3$): δ (ppm) 8.76 (s, 1H), 8.53 (s, 1H), 8.06 (d, J = 6.0 Hz, 1H), 7.86−7.80 (m, 4H), 7.67 (d, J = 6.0 Hz, 2H), 7.17 (d, J = 6.6 Hz, 1H), 7.11 (d, J = 6.0 Hz, 1H), 6.97 (t, J = 6.0 Hz, 1H), 6.87 (t, J = 6.0 Hz, 1H), 6.81 (t, J = 6.0 Hz, 1H), 6.71 (t, J = 6.0 Hz, 1H), 6.58 (s, 1H), 6.48 (t, J = 3.6 Hz, 1H), 6.33 (d, J = 1.2 Hz, 1H), 2.19 (s, 3H), 2.15 (s, 3H). ^{13}C NMR (300 MHz, $CDCl_3$): δ (ppm) 174. 07, 152.09, 145.36, 144.21, 144.10, 138.39, 137.30, 135.70, 134.55, 134.34, 132.30, 131.21, 130.31, 129.67, 128.77, 128.57, 127.75, 126.43, 125.88, 125.54, 125.08, 124.76, 122.16, 121.83, 118.12, 117.93, 110.78, 110.587, 9.65, 9.56. ESI-MS: *m/z* 680.5 [M + H$^+$]. Anal. Calcd for $C_{30}H_{24}IrN_5O_2 \cdot 0.5H_2O$: C 52.39; H 3.66; N 10.18. Found: C 52.01; H 3.59; N 10.11.

(1*p*3,5*dmpz*)$_2$Ir3*iq* (4). ^{1}H NMR (300 MHz, $CDCl_3$): δ (ppm) 8.62 (s, 1H), 8.52 (s, 1H), 8.22 (d, J = 6.0 Hz, 1H), 7.93−7.88 (m, 2H), 7.74 (t, J = 7.91 Hz, 1H), 7.55−7,44 (m, 3H), 6.84 (t, J = 7.2 Hz, 1H), 6.73 (t, J = 7.5 Hz, 1H), 6.63 (t, J = 7.5 Hz, 1H), 6.53 (t, J = 7.5 Hz, 1H), 6.27−5.22 (m, 3H), 2.39 (s, 6H), 1.55 (s, 6H). ^{13}C NMR (300 MHz, $CDCl_3$): δ (ppm) 174.09, 151.90, 150.59, 148.99, 146.11, 145.82, 145.63, 140.30, 140.27, 140.22, 135.58, 134.94, 134.42, 132.18, 131.84, 130.49, 129.98, 129.58, 128.59, 127.72, 126.13, 125.13, 124.65, 122.21, 121.73, 112.11, 109.72, 109.63, 14.83, 14.59, 13.06, 12.67. ESI-MS: *m/z* 708.7 [M + H$^+$]. Anal. Calcd for $C_{32}H_{28}IrN_5O_2$: C 54.38; H 3.99; N 9.91. Found: C 54.47; H 4.23; N 9.28.

(4*tpz*)$_2$Ir3*iq* (5). ^{1}H NMR (300 MHz, $CDCl_3$): δ (ppm) 8.73 (s, 1H), 8.52 (s, 1H), 8.03−8.00 (m, 3H), 7.81 (t, J = 4.5 Hz, 3H), 7.66 (t, J = 9.1 Hz, 1H), 7.13 (d, J = 6.0 Hz, 1H), 7.07 (d, J = 4.5 Hz, 1H), 6.78−6.74 (m, 2H), 6.69 (d, J = 6.0 Hz, 1H),

6.54 (d, J = 2.4 Hz, 1H), 6.43 (t, J = 2.1 Hz, 1H), 6.21 (s, 1H), 6.08 (s, 1H) 2.17 (s, 3H), 2.13 (s, 3H). ^{13}C NMR (300 MHz, $CDCl_3$): δ (ppm) 174.04, 152.08, 145.31, 141.81, 141.78, 137.89, 136.95, 135.78, 135.68, 135.35, 134.99, 132.34, 131.06, 130.28, 129.67, 128.74, 128.57, 127.79, 126.48, 125.81, 125.55, 123.04, 122.68, 110.84, 110.67, 107.25, 107.19, 106.277, 21.61, 21.54. ESI-MS: *m/z* 680.7 [M + H$^+$]. Anal. Calcd for $C_{30}H_{24}IrN_5O_2\cdot H_2O$: C 51.71; H 3.76; N 10.05. Found: C 51.79; H 3.68; N 9.80.

(5*tpz*)$_2$Ir3*iq* (6). ^{1}H NMR (300 MHz, $CDCl_3$): δ (ppm) 8.75 (s, 1H), 8.57 (s, 1H), 8.03 (t, J = 3.6 Hz, 3H), 7.83 (t, J = 4.2 Hz, 3H), 7.72−7.68 (m, 1H), 7.07 (s, 1H), 7.02 (s, 1H), 6.76 (d, J = 2.1 Hz, 1H), 6.64(d, J = 4.5 Hz, 1H), 6.58−6.56 (m, 2H), 6.45 (d, J = 2.3 Hz, 1H), 6.30 (d, J = 7.4 Hz, 1H), 6.15 (d, J = 7.5 Hz, 1H), 2.30 (s, 3H), 2.23 (s, 3H). ^{13}C NMR (300 MHz, $CDCl_3$): δ (ppm) 174.13, 152.13, 145.36, 143.86, 143.78, 138.22, 137.20, 135.67, 134.18, 133.93, 132.32, 131.60, 131.27, 130.31, 129.68, 128.57, 127.73, 127.40, 127.04, 126.82, 126.46, 125.99, 125.73, 124.12, 112.12, 111.89, 107.37, 107.25, 21.35, 21.26. ESI-MS: *m/z* 680.7 [M + H$^+$]. Anal. Calcd for $C_{30}H_{24}IrN_5O_2\cdot H_2O$: C 51.71; H 3.76; N 10.05. Found: C 51.29; H 3.61; N 9.92.

(6*tpz*)$_2$Ir3*iq* (7). ^{1}H NMR (300 MHz, $CDCl_3$): δ (ppm) 8.76 (s, 1H), 8.50 (s, 1H), 8.33 (t, J = 3.1 Hz, 2H), 8.03 (d, J = 6.2 Hz, 1H), 7.91 (d, J = 3.0 Hz, 1H), 7.81 (t, J = 3.2 Hz, 2H), 7.72−7.61 (m, 1H), 6.80−6.77 (m, 2H). 6.71−6.68 (m, 2H), 6.63−6.60 (m, 2H), 6.48 (t, J = 3.0 Hz, 1H), 6.26 (d, J = 6.0 Hz, 1H), 6.04 (d, J = 6.2 Hz, 1H), 2.66 (s, 3H), 2.60 (s, 3H). ^{13}C NMR (300 MHz, $CDCl_3$): δ (ppm) 174.06, 151.92, 143.24, 143.20, 137.66, 136.65, 135.71, 133.26, 132.52, 132.39, 132.36, 131.13, 130.70, 130.43, 130.43, 130.31, 129.73, 128.60, 127.79, 126.76, 126.55, 126.34, 125.86, 125.44, 121.61, 121.29, 107.51, 107.33, 21.90, 21.86. ESI-MS: *m/z* 680.7 [M + H$^+$]. Anal. Calcd for $C_{30}H_{24}IrN_5O_2\cdot 0.5H_2O$: C 52.39; H 3.66; N 10.18. Found: C 52.59; H 3.85; N 9.91.

(4*m*5*tpz*)$_2$Ir3*iq* (8). ^{1}H NMR (300 MHz, $CDCl_3$): δ (ppm) 8.82−8.70 (m, 1H), 8.09−8.05 (m, 1H), 7.90−7.81 (m, 5H), 7.80−7.62 (m, 3H), 6.99−6.95 (m, 1H), 6.86 (s, 1H), 6.54 (s, 1H), 6.36−6.31(m, 2H), 5.87 (d, J = 7.5 Hz, 1H), 2.25 (s, 6H), 2.14 (s, 6H). ^{13}C NMR (300 MHz, $CDCl_3$): δ (ppm) 174.09, 152.07, 145.50, 144.15, 144.05, 138.28, 137.19, 135.65, 134.14, 133.93, 132.17, 131.37, 131.03, 130.30, 129.54, 128.55, 127.72, 126.88, 126.58, 126.31, 124.85, 124.51, 124.20, 124.12, 117.92, 117.73, 111.75, 111.55, 21.37, 21.28, 9.68. 9.58. ESI-MS: *m/z* 708.7 [M + H$^+$]. Anal. Calcd for $C_{32}H_{28}IrN_5O_2\cdot 0.5H_2O$: C 53.69; H 4.08; N 9.78. Found: C 53.25; H 4.12; N 9.62.

(*ppz*)$_2$Ir1*iq* (9). ^{1}H NMR (300 MHz, $CDCl_3$): δ (ppm) 10.26−10.24 (m, 1H), 8.07 (m, 2H), 7.86−7.84 (d, J = 3 Hz, 1H), 7.82−7.78 (m, 4H), 7.65 (d, J = 3 Hz, 1H), 7.24−7.18 (m, 2H), 6.96 (t, J = 6 Hz, 1H), 6.89 (t, J = 6 Hz, 1H), 6.80−6.73 (m, 3H), 6.61 (t, J = 1.5 Hz, 1H), 6.47 (s, J = 2.4 Hz, 1H), 6.41 (d, J = 3.0 Hz, 1H) 6.27 (d, J = 3.0 Hz, 1H). ESI-MS: *m/z* 652.5 [M + H$^+$]. Anal. Calcd for $C_{28}H_{20}IrN_5O_2\cdot 0.5H_2O$: C 50.98; H 3.21; N 10.76. Found: C 51.15; H 3.38; N 9.89.

(3*mppz*)$_2$Ir1*iq* (10). ^{1}H NMR (300 MHz, $CDCl_3$): δ (ppm) 10.17−10.13 (m, 1H), 7.96−7.94 (m, 2H), 7.85−7.79 (m, 4H), 7.69 (d, J = 3.6 Hz, 1H) 7.23−7.11 (m, 2H), 6.98 (t, J = 4.5 Hz, 1H), 6.90 (d, J = 3.6 Hz, 1H), 6.82−6.65 (m, 2H), 6.44 (d, J = 3 Hz, 1H), 6.29 (dd, J = 4.7 Hz, 3,3 Hz, 2H), 6.19 (d, J = 7.3 Hz, 1H), 2.48 (s, 3H), 1.57(s, 3H). ESI-MS: *m/z* 680.7 [M + H$^+$]. Anal. Calcd for $C_{30}H_{24}IrN_5O_2$: C 53.09; H 3.56; N 10.32. Found: C 53.07; H 3.72; N 10.01.

(4*mppz*)$_2$Ir1*iq* (11). ^{1}H NMR (300 MHz, $CDCl_3$): δ (ppm) 10.29−10.26 (m, 1H), 7.91 (d, J = 6.0 Hz, 1H), 7.84−7.78 (m, 5H), 7.63 (d, J = 6.0 Hz, 2H), 7.15−7.10 (m, 2H), 7.00−6.88 (m, 2H), 6.77 (t, J = 1.0 Hz, 1H), 6.71 (t, J = 1.0 Hz, 1H), 6.55 (s, 1H), 6.44 (d, J = 3.0 Hz, 1H), 6.30 (d, J = 3.0 Hz, 1H), 2.15 (s, 3H), 2.05 (s, 3H). ^{13}C NMR (300 MHz, $CDCl_3$): δ (ppm) 174.06, 151.03, 144.10, 143.97, 141.37, 140.61, 138.39, 137.40, 137.01, 134.55, 134.27, 132.60, 131.83, 129.59, 128.85, 126.78, 126.17, 125.86, 125.59, 125.02, 124.70, 122.14, 121.71, 118.09, 117.98, 116.81, 110.78, 110.61, 9.71, 9.60. ESI-MS: *m/z* 680.5 [M + H$^+$]. Anal. Calcd for $C_{30}H_{24}IrN_5O_2\cdot 3H_2O$: C 49.17; H 4.13; N 9.56. Found: C 49.29; H 3.55; N 9.26.

(1*p*3,5*dmpz*)$_2$Ir1*iq* (12). ^{1}H NMR (300 MHz, $CDCl_3$): δ (ppm) 10.27−10.24 (m, 1H), 7.78−7.73 (m, 4H), 7.60 (d, J = 6.0 Hz, 1H), 7.39 (d, J = 9.0 Hz, 1H), 7.34 (d, J = 6.0 Hz, 1H), 6.96 (t, J = 3.02 Hz, 1H), 6.86 (t, J = 3.0 Hz, 1H), 6.75 (t, J = 3.0 Hz, 1H), 6.67 (t, J = 3.0 Hz, 1H), 6.55 (d, J = 4.0 Hz, 1H), 6.21 (d, J = 4.0 Hz, 1H), 6.02 (d, J = 4.1 Hz, 2H), 2.82 (s, 3H), 2.80 (s, 3H), 2.41 (s, 3H), 1.53 (s, 3H). ^{13}C NMR (300 MHz, $CDCl_3$): δ (ppm) 174.27, 151.32, 149.00, 146.06, 145.62, 141.25, 141.10, 140.21, 136.92, 134.91, 134.19, 131.97, 131.18, 129.72, 129.59, 129.36, 126.78, 126.64, 126.53, 126.35, 125.05, 124.68, 122.21, 121.60, 112.24, 112.06, 109.22, 109.13, 14.70, 14.31, 12.81, 12.73. ESI-MS: *m/z* 708.7 [M + H$^+$]. Anal. Calcd for $C_{32}H_{28}IrN_5O_2$: C 54.38; H 3.99; N 9.91. Found: C 54.14; H 4.01; N 9.65.

(4*tpz*)$_2$Ir1*iq* (13). ^{1}H NMR (300 MHz, $CDCl_3$): δ (ppm) 10.26−10.24 (m, 1H), 8.01 (d, J = 3.0 Hz, 2H), 7.90 (d, J = 6.0 Hz, 1H), 7.80−7.75 (m, 4H), 7.61 (d, J = 6.0 Hz, 1H), 7.12 (d, J = 4.5 Hz, 1H), 7.07 (d, J = 4.5 Hz, 1H), 6.78 (d, J = 9.0 Hz, 1H), 6.70−6.63 (m, 2H), 6.53 (d, J = 1.1 Hz, 1H), 6.42 (d, J = 1.1 Hz, 1H), 6.17 (d, J = 1.1 Hz, 1H), 6.06 (d, J = 1.1 Hz, 1H), 2.15 (s, 3H), 2.08 (s, 3H). ^{13}C NMR (300 MHz, $CDCl_3$): δ (ppm) 174.12, 151.19, 141.39, 141.27, 137.98, 137.81, 137.09, 136.97, 135.83, 135.76, 135.41, 131.22, 129.98, 129.84, 129.67, 129.53, 126.84, 126.68, 125.80, 125.71, 125.56, 125.46, 123.08, 122.96, 110.94, 110.75, 107.27, 107.21, 21.96, 21.13. ESI-MS: *m/z* 680.6 [M + H$^+$]. Anal. Calcd for $C_{30}H_{24}IrN_5O_2\cdot 1.5H_2O$): C 50.41; H 3.95; N 9.80. Found: C 50.70; H 3.38; N 9.61.

(5*tpz*)$_2$Ir1*iq* (14). ^{1}H NMR (300 MHz, $CDCl_3$): δ (ppm) 10.27−10.24 (m, 1H), 8.04 (d, J = 3.0 Hz, 2H), 7.95 (d, J = 6.1 Hz, 1H) 7.83−7.79 (m, 4H), 7.63 (d, J = 3.0 Hz, 1H), 7.08(s, 1H), 7.03(s, 1H), 6.73 (d, J = 2.1 Hz, 1H), 6.63 (d, J = 2.2 Hz, 1H), 6.56 (d, J = 2.5 Hz, 2H), 6.45 (t, J = 2.4 Hz, 1H), 6.27 (d, J = 3.8 Hz, 1H), 6.13 (d, J = 3.8 Hz, 1H), 2.29 (s, 3H), 2.23 (s, 3H). ^{13}C NMR (300 MHz, $CDCl_3$): δ (ppm) 174.06, 151.12, 143.84, 143.71, 141.37, 140.46, 138.24, 137.31, 137.02, 134.23, 133.95, 132.41, 131.84, 131.58, 131.18, 129.99, 129.58, 128.89, 127.40, 127.11, 126.75, 126.13, 125.91, 125.68, 112.13, 111.92, 107.35, 107.30, 21.32, 21.25. ESI-MS: *m/z* 680.6 [M + H$^+$]. Anal. Calcd for $C_{30}H_{24}IrN_5O_2$: C 53.09; H 3.56; N 10.32. Found: C 53.33; H 3.81; N 9.50.

(6*tpz*)$_2$Ir1*iq* (15). ^{1}H NMR (300 MHz, $CDCl_3$): δ (ppm) 10.26−10.24 (m, 1H), 8.32 (d, J = 1.2 Hz, 2H), 7.88−7.77 (m, 5H), 7.61 (d, J = 6.4 Hz, 1H), 6.76 (d, J = 3.0 Hz, 2H), 6.67−6.58 (m, 4H), 6.47 (t, J = 3.0 Hz, 1H), 6.21 (d, J = 4.0 Hz, 1H), 6.05 (d, J = 4.0 Hz, 1H), 2.64 (s, 3H), 2.59 (s, 3H). ^{13}C NMR (300 MHz, $CDCl_3$): δ (ppm) 174.06, 151.92, 143.24, 143.20, 137.66, 136.65, 135.71, 133.40, 132.52, 132.39, 131.13, 130.70, 130.43, 130.43, 130.31, 129.73, 128.60, 127.79, 126.76, 126.55, 126.34, 125.86, 125.44, 121.61, 121.29, 107.51, 107.33, 104.82, 21.90, 21.86. ESI-MS: *m/z* 680.6 [M + H$^+$]. Anal. Calcd for $C_{30}H_{24}IrN_5O_2\cdot 0.5H_2O$): C 52.39; H 3.66; N 10.11. Found: C 52.60; H 3.67; N 9.91.

(4*m*5*tpz*)$_2$Ir1*iq* (16). ^{1}H NMR (300 MHz, $CDCl_3$): δ (ppm) 10.27−10.24 (m, 1H), 7.96−7.76 (m, 6H), 7.71 (s, 1H), 7.62 (s, 1H), 6.98−6.86 (m, 3H), 6.56−6.52 (m, 1H), 6.36−6.29 (m, 1H), 6.18 (d, J = 6.0 Hz, 1H), 5.86 (d, J = 9.0 Hz, 1H), 2.27 (s, 6H), 2.12 (s, 6H). ^{13}C NMR (300 MHz, $CDCl_3$): δ (ppm) 174.02, 152.12, 144.07, 143.93, 141.44, 138.30, 137.29, 136.95, 134.14, 133.88, 131.72, 131.36, 130.96, 129.98, 129.51, 128.86, 126.94, 126.87, 126.77, 126.63, 126.07, 125.11, 124.82, 124.48, 117.91, 117.79, 111.77, 111.60, 21.34, 21.28, 9.71, 9.60. ESI-MS: *m/z* 708.6 [M + H$^+$]. Anal. Calcd for $C_{32}H_{28}IrN_5O_2$: C 54.38; H 3.99; N 9.91. Found: C 54.38; H 3.84; N 9.42.

Acknowledgment. We thank the CMDS (KOSEF) and Sumsung SDI-SNU Display Innovation Program for financial support. T.-H.K, H.S.C., and M.K.K. are recipients of a BK 21 fellowship.

Supporting Information Available: Electrochemical data, DFT calculations, PL spectrum, and transient PL spectrum at 77 K and X-ray crystallographic data including CIF files for **1** and **11**. This material is available free of charge via the Internet at http://pubs.acs.org.

OM049419E